

lengths determined by EXAFS with the X-ray distances shows excellent agreement. Little change in first coordination sphere bond lengths would be expected when  $\text{PMe}_2\text{Ph}$  is replaced with  $\text{PEt}_3$ ; thus, the similar results obtained for  $[\text{Ni}(\text{PEt}_3)_2\text{Br}_3]$  can be viewed with some confidence.

**Chloride Complexes.** Distinguishing phosphorus from chlorine in EXAFS analyses often presents difficulties because of the very similar backscattering powers of the two elements. Fits produced by using a single shell of phosphorus or chlorine atoms were therefore compared to that derived from the two-shell model. For both complexes, a significant decrease<sup>17</sup> in  $R$  factor (12%) was observed for the two-shell fit, and no unacceptably high correlations between the two shells were observed. Thus, the bond lengths quoted in Table II are believed to be reliable to within  $\pm 0.03$  Å.

**Acknowledgment.** We thank the SERC (J.M.C. and M.D.S.) and BP Research (J.M.C.) for support, the Director of The Daresbury Laboratory for the provision of facilities, and Professor C. D. Garner and Dr. D. A. Rice for the use of the Varian Cary 2300 and Beckman Acta spectrometers, respectively.

Contribution from the Department of Chemistry  
and Biochemistry, The University of Texas,  
Austin, Texas 78712

### Synthesis and Characterization of a Tetranuclear Iron(III) Complex Derived from a New *m*-Xylyl-Bridged Tetraimidazole Ligand

Jonathan L. Sessler,\* Jeffrey D. Hugdahl, Vincent Lynch, and Brian Davis

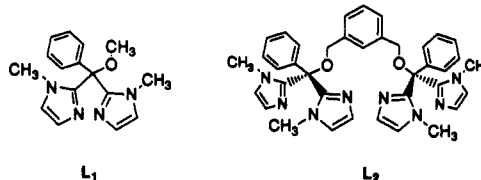
Received May 30, 1990

Binuclear iron-oxo centers have been found to be a common structural element at the active sites of numerous proteins, including hemerythrin,<sup>1-4</sup> purple acid phosphatase,<sup>5</sup> ribonucleotide reductase,<sup>6</sup> ruberythrin,<sup>7</sup> and methane monooxygenase.<sup>8</sup> These centers perform a wide variety of important biological processes, including oxygen transport, methane oxidation, and oxygen atom transfer. While many models of the bimetallic site exist, relatively few of the models employ imidazoles as the sole N-donors.<sup>9,10</sup> Such biomimetic models may ultimately prove important in reproducing the chemical and physical properties of the histidine-

Table I. Crystallographic Data for 2

chem formula	$\text{C}_{90}\text{H}_{102}\text{N}_{16}\text{O}_{26}\text{Fe}_4\text{Cl}_6$	space group	$P2_1/n$ (No. 14)
fw	2260.00	$T, ^\circ\text{C}$	-80
$a, \text{Å}$	14.192 (3)	$\rho_{\text{calc}}, \text{g cm}^{-3}$	1.49
$b, \text{Å}$	16.557 (3)	$\mu, \text{cm}^{-1}$	8.029
$c, \text{Å}$	21.856 (6)	transm coeff	0.8012-0.9376
$\beta, \text{deg}$	101.25 (2)	$R(F_o)$	0.0747
$V, \text{Å}^3$	5037 (2)	$R_w(F_o)$	0.0656
$Z$	2		

dominated cores found in the protein systems.<sup>11</sup> Recently, Lippard et al. has succeeded in crystallizing both an unsymmetrical iron(II) and a symmetrical iron(III) dimer utilizing the diimidazole ligand ( $L_1$ ) as the sole capping subunit.<sup>9</sup> This success suggests that further studies with related imidazole-containing ligands might also be informative. In this note, we report the synthesis of a new xylyl-bridged tetraimidazole ligand,  $L_2$ , and the results of iron



binding and X-ray structural studies carried out with this system. We have found that this new ligand, with its rigid xylyl bridge, serves to stabilize the formation of a tetranuclear  $\mu$ -oxo iron(III) complex in the solid state.<sup>12</sup>

### Experimental Section

NMR spectra were obtained in  $\text{CDCl}_3$  with  $\text{Me}_4\text{Si}$  as an internal standard and recorded on a General Electric QE-300 spectrometer. Chemical ionization mass spectrometric analyses (CI MS) were made by using a Finnigan MAT 4023. Infrared spectra were recorded, as KBr pellets, from 4000 to  $400 \text{ cm}^{-1}$  on a Bio-Rad FTS-40 spectrophotometer. Electronic spectra were recorded in chloroform on a Beckman DU-7 spectrophotometer.

**Bis(1-methylimidazol-2-yl)phenylcarbinol (1).** A solution of *N*-methylimidazole (5.0 g, 60.9 mmol) in 200 mL of THF under nitrogen was cooled to  $-78^\circ\text{C}$  and treated with 42 mL of 1.6 M *n*-butyllithium in hexanes for 1 h. Benzoyl chloride (4.28 g, 30.4 mmol) was dissolved in 25 mL of THF and added dropwise. The solution was warmed to room temperature over 4 h, and 50 mL of water was added. THF was removed in vacuo. The aqueous solution was extracted with methylene chloride, dried over  $\text{MgSO}_4$ , filtered, and concentrated. Addition of ether to the methylene chloride solution afforded a white precipitate that was filtered and dried, affording 1 (6.3 g), which was used without further purification: yield 78%.  $^1\text{H NMR}$ :  $\delta$  3.39 (6 H, s,  $\text{NCH}_3$ ), 6.5 (1 H, br,  $-\text{OH}$ ), 6.88 (2 H, s,  $\text{Im}4\text{H}$ ), 6.95 (2 H, s,  $\text{Im}5\text{H}$ ), 7.09 (2 H, m, phenyl), 7.34 (3 H, m, phenyl).  $^{13}\text{C NMR}$ :  $\delta$  30.71, 74.98, 123.49, 125.98, 127.45, 128.36, 148.45. CI MS  $m/e$  269 ( $\text{MH}^+$ ).

**1,3-Bis((bis(1-methylimidazol-2-yl)phenylmethoxy)methyl)benzene ( $L_2$ ).** A stirred solution of 1 (1.52 g, 5.67 mmol) in 50 mL of dry dimethylformamide (DMF) under nitrogen was treated with sodium hydride (156 mg, 6.5 mmol).  $\alpha, \alpha'$ -Dibromo-*m*-xylene (0.75 g, 2.83 mmol) was added all at once, and the solution was stirred overnight. The DMF was removed in vacuo, and the resulting solid was dissolved in 20 mL of water and extracted chloroform. The chloroform extracts were dried over magnesium sulfate, filtered, and removed in vacuo, leaving a white foam ( $L_2$ ) (1.70 g): yield 94%.  $^1\text{H NMR}$ :  $\delta$  3.34 (12 H, s,  $\text{NCH}_3$ ), 4.42 (4 H, s,  $\text{PhCH}_2\text{O}-$ ), 6.78 (4 H, s,  $\text{Im}4\text{H}$ ), 6.97 (4 H, s,  $\text{Im}5\text{H}$ ), 7.30 (10 H, m, phenyl), 7.53 (4 H, d, phenyl).  $^{13}\text{C NMR}$ :  $\delta$  34.20, 67.47, 81.54, 122.84, 125.58, 126.40, 126.45, 127.49, 127.55, 127.83, 127.94, 138.03, 138.25, 146.32. IR (KBr,  $\text{cm}^{-1}$ , selected peaks): 3386 (w), 3102 (m), 1677 (m), 1486 (s), 1446 (s), 1400 (m), 1279 (s), 1057 (s), 904 (m), 893 (m), 754 (vs), 721 (s), 700 (s). CI MS:  $m/e$  639 ( $\text{MH}^+$ ). HR CI MS: found,  $m/e$  638.312026; calcd,  $m/e$  638.311773.

**Preparation of  $[\text{Fe}_2(L_2)(\mu\text{-O})(\mu\text{-HCO}_2)_2(\text{HCO}_2)_2]_2$  (2).** The metal complex has been prepared by two methods.

- (1) Wilkins, R. G.; Harrington, P. C. *Adv. Inorg. Biochem.* **1983**, *5*, 51-86.
- (2) Sheriff, S.; Hendrickson, W. A.; Smith, J. L. *J. Mol. Biol.* **1987**, *197*, 273-296.
- (3) Garbett, K.; Darnall, D. W.; Klotz, I. M.; Williams, R. J. P. *Arch. Biochem. Biophys.* **1969**, *135*, 419-434.
- (4) Wilkins, P. C.; Wilkins, R. G. *Coord. Chem. Rev.* **1987**, *79*, 195-214.
- (5) Antanaitis, B. C.; Aisen, P. *Adv. Inorg. Biochem.* **1983**, *5*, 111-136.
- (6) Sjöberg, B.-M.; Graslund, A. *Adv. Inorg. Biochem.* **1983**, *5*, 87-110.
- (7) LeGall, J.; Prickril, B. C.; Moura, I.; Xavier, A. V.; Moura, J. J. G.; Huynh, B.-H. *Biochemistry* **1988**, *27*, 1636-1642.
- (8) Fox, B. G.; Froland, W. A.; Dege, J. E.; Lipscomb, J. D. *J. Biol. Chem.* **1989**, *264*, 10023-10033.
- (9) Tolman, W. B.; Bino, A.; Lippard, S. J. *J. Am. Chem. Soc.* **1989**, *111*, 8522-8523.
- (10) Structurally characterized iron complexes employing imidazole or benzimidazole in addition to other nitrogen donors have been reported: (a) Suzuki, M.; Oshio, H.; Uehara, A.; Endo, K.; Yanaga, M.; Kida, S.; Saito, K. *Bull. Chem. Soc. Jpn.* **1988**, *61*, 3907-3913. (b) Gomez-Romero, P.; Casan-Pastor, J.; Ben-Hussein, A.; Jameson, G. B. *J. Am. Chem. Soc.* **1988**, *110*, 1988-1990. (c) Mashuta, M. S.; Webb, R. J.; Oberhausen, K. J.; Richardson, J. F.; Buchanan, R. M.; Hendrickson, D. N. *J. Am. Chem. Soc.* **1989**, *111*, 2745-2746. (d) Adams, H.; Bailey, N. A.; Crane, J. D.; Fenton, D. E.; Latour, J.-M.; Williams, J. M. *J. Chem. Soc., Dalton Trans.* **1990**, 1727-1735.

(11) Tolman, W. B.; Rardin, R. L.; Lippard, S. J. *J. Am. Chem. Soc.* **1989**, *111*, 4532-4533.

(12) Two similar complexes have been reported: (a) Toftlund, H.; Murray, K. S.; Zwack, P. R.; Taylor, L. F.; Anderson, O. P. *J. Chem. Soc., Chem. Commun.* **1986**, 191-193. (b) Sessler, J. L.; Sibert, J. W.; Lynch, V. *Inorg. Chem.* **1990**, *29*, 4143-4146.

**Table II.** Atomic Coordinates ( $\times 10^4$ ) and Equivalent Isotropic Displacement Coefficients ( $\text{\AA}^2 \times 10^3$ )

atom	x	y	z	$U^a$
Fe(1)	3223 (2)	-88 (1)	963 (1)	31 (1)
Fe(2)	3570 (2)	1809 (1)	1246 (1)	31 (1)
N(1)	2678 (8)	-1269 (7)	1212 (5)	32 (5)
C(2)	3152 (10)	-1947 (8)	1412 (6)	26 (6)
N(3)	2530 (9)	-2505 (7)	1571 (5)	38 (5)
C(4)	1664 (12)	-2148 (9)	1476 (7)	53 (8)
C(5)	1733 (10)	-1397 (9)	1246 (6)	35 (6)
C(6)	2715 (11)	-3318 (8)	1830 (7)	58 (8)
N(7)	4477 (8)	-780 (7)	974 (5)	30 (5)
C(8)	4731 (10)	-1544 (8)	1110 (6)	31 (6)
N(9)	5583 (8)	-1699 (7)	942 (5)	38 (5)
C(10)	5858 (10)	-1024 (8)	667 (7)	36 (6)
C(11)	5210 (10)	-471 (8)	709 (6)	28 (6)
C(12)	6154 (10)	-2449 (8)	1028 (7)	59 (7)
C(13)	4698 (9)	-2365 (8)	2060 (7)	23 (6)
C(14)	4783 (9)	-1758 (9)	2497 (7)	34 (6)
C(15)	5181 (10)	-1893 (9)	3109 (7)	41 (6)
C(16)	5552 (10)	-2648 (10)	3307 (8)	50 (7)
C(17)	5484 (11)	-3247 (10)	2862 (8)	52 (7)
C(18)	5069 (10)	-3114 (9)	2245 (7)	35 (6)
C(19)	4194 (10)	-2192 (8)	1405 (6)	21 (5)
O(20)	4153 (6)	-2912 (5)	1033 (4)	32 (4)
C(21)	3657 (11)	-2834 (8)	408 (7)	46 (7)
C(22)	3717 (11)	-3599 (9)	45 (6)	34 (6)
C(23)	4445 (10)	-3698 (8)	-301 (7)	41 (6)
C(24)	4494 (11)	-4384 (8)	-640 (7)	37 (6)
C(25)	3844 (11)	-5002 (8)	-628 (6)	40 (6)
C(26)	3094 (12)	-4908 (10)	-292 (7)	53 (7)
C(27)	3054 (11)	-4218 (10)	46 (7)	50 (7)
C(28)	5201 (10)	-4453 (8)	-1067 (7)	36 (6)
O(29)	4789 (6)	-4347 (5)	-1703 (4)	32 (4)
C(30)	4959 (10)	-3600 (8)	-1972 (7)	35 (7)
N(31)	6614 (8)	-2908 (6)	-1781 (5)	34 (5)
C(32)	6013 (10)	-3497 (8)	-1973 (6)	23 (6)
N(33)	6491 (9)	-4096 (7)	-2220 (5)	38 (5)
C(34)	7431 (11)	-3850 (9)	-2180 (6)	41 (7)
C(35)	7498 (11)	-3118 (9)	-1908 (6)	41 (7)
C(36)	6143 (11)	-4874 (8)	-2507 (7)	59 (7)
N(37)	5016 (8)	-2267 (6)	-1355 (5)	31 (5)
C(38)	4567 (10)	-2912 (8)	-1636 (6)	28 (6)
N(39)	3605 (8)	-2882 (7)	-1606 (5)	31 (5)
C(40)	3490 (11)	-2195 (8)	-1277 (6)	39 (7)
C(41)	4337 (10)	-1822 (9)	-1131 (7)	37 (6)
C(42)	2833 (10)	-3460 (8)	-1837 (7)	59 (7)
C(43)	4424 (11)	-3621 (9)	-2645 (7)	36 (7)
C(44)	3906 (11)	-4285 (9)	-2912 (8)	46 (7)
C(45)	3464 (12)	-4259 (11)	-3533 (9)	65 (9)
C(46)	3538 (13)	-3584 (13)	-3880 (8)	69 (9)
C(47)	4013 (12)	-2905 (11)	-3609 (9)	60 (8)
C(48)	4459 (10)	-2926 (10)	-2993 (7)	39 (7)
O(49)	3775 (6)	875 (5)	862 (4)	27 (4)
O(50)	2763 (8)	-338 (6)	57 (6)	60 (5)
C(51)	2242 (25)	-802 (12)	-227 (11)	171 (19)
O(52)	2022 (9)	-1095 (7)	-711 (6)	85 (6)
O(53)	1860 (7)	309 (6)	995 (5)	52 (5)
C(54)	1617 (12)	1006 (11)	1129 (7)	58 (9)
O(55)	2157 (7)	1602 (6)	1290 (5)	46 (5)
O(56)	3550 (7)	16 (6)	1958 (4)	37 (4)
C(57)	3873 (10)	597 (9)	2294 (7)	39 (7)
O(58)	3988 (7)	1322 (5)	2139 (4)	38 (4)
O(59)	3162 (7)	2473 (6)	460 (5)	41 (4)
C(60)	2430 (14)	2863 (10)	300 (9)	62 (9)
O(61)	2099 (8)	3232 (6)	-179 (5)	58 (5)
C(1A)	8579 (11)	5817 (10)	2337 (8)	66 (8)
Cl(1)	8699 (3)	4973 (3)	2811 (2)	89 (2)
Cl(2)	7441 (4)	6236 (3)	2264 (3)	94 (3)
Cl(3)	8813 (4)	5570 (4)	1601 (3)	121 (3)
O(1C)	192 (11)	3480 (10)	-349 (7)	127 (8)
C(2C)	-202 (16)	2914 (15)	43 (9)	159 (16)
O(1B)	-1048 (11)	4455 (11)	-1030 (7)	132 (9)
C(2B)	-988 (19)	5178 (13)	-776 (11)	157 (16)

<sup>a</sup> Equivalent isotropic  $U$  defined as one-third of the trace of the orthogonalized  $U_{ij}$  tensor.

(a) To a stirred solution of  $L_2$  (0.100 g, 0.156 mmol) in 10 mL of methanol under argon was added ferrous formate dihydrate<sup>13</sup> (0.057 g,

0.313 mmol). The solution was exposed to air overnight; the methanol was removed in vacuo giving a green solid.

(b) To a stirred solution of  $L_2$  (0.084 g, 0.132 mmol) in 10 mL of methanol were added ferric chloride (0.071 g, 0.264 mmol) and ammonium formate (0.040 g, 0.635 mmol). The solution immediately turned green, and a small amount of white precipitate appeared. The methanol was removed, and 50 mL of chloroform was added. The resulting precipitate (found to be ammonium chloride and excess ammonium formate) was filtered off, and the chloroform was removed in vacuo, giving a green solid.

Both solids were identical by visible and IR spectra. Green crystals of the iron complex were obtained by vapor diffusion of ether into a chloroform/methanol solution of **2**: yield 71%. IR (KBr,  $\text{cm}^{-1}$ , selected peaks): 3429 (w), 3133 (m), 1653 (s), 1616 (vs), 1591 (vs), 1499 (s), 1356 (m), 1282 (m), 1063 (m), 898 (m), 761 (s), 724 (m), 705 (m). UV-vis: see Table III. Anal. Calcd. for  $C_{90}H_{102}Cl_6Fe_4N_{16}O_2$ : C, 47.83; H, 4.55; N, 9.92. Found: C, 47.95; H, 4.48; N, 9.99. Complex **2** was further characterized by X-ray crystallography (see below and Figure 1).

**Crystal Structure of  $[\text{Fe}_2\text{O}_2(\text{C}_7\text{H}_6\text{N}_6\text{O}_4)(\text{CHO}_2)_2] \cdot 2\text{CHCl}_3 \cdot 4\text{CH}_3\text{OH}$  (**2**).** Structure solutions and refinement were effected by using the procedure, programs, and parameters, and parameters reported earlier.<sup>14</sup> The data crystal was a green plate of approximate dimensions:  $0.09 \times 0.31 \times 0.32$  mm. Data were collected at  $-80$  °C on a Nicolet R3 diffractometer, equipped with a graphite monochromator and a Nicolet LT-2 low-temperature delivery system (Table I). The crystal system is monoclinic and the space group is  $P2_1/n$  (No. 14), as uniquely determined from systematically absent reflections. The structure was solved by direct methods and refined by full-matrix least-squares procedures with anisotropic thermal parameters for the non-hydrogen atoms. Table II lists the final atomic coordinates and isotropic thermal parameters for the non-hydrogen atoms. The H atoms were calculated in idealized positions and refined with isotropic thermal parameters riding at  $1.2U_{eq}$  of the relevant atom. No H atoms for the solvent methanol oxygen atoms were included in the refinement.

## Results and Discussion

**Ligand Design and Synthesis.** The wide variety of biological processes mediated by the binuclear iron core has prompted the design and synthesis of numerous models.<sup>15</sup> Many of these models rely on simple tridentate capping ligands, and the model complexes formed from these ligands provide accurate spectroscopic and structural depictions of the protein's diiron core. However, these simple systems lack the necessary stability to mimic the chemical reactivity. Covalently linking these simple ligand systems with rigid bridges may provide the additional stability necessary to model more fully the natural systems. Our recent interest in covalently linked triazacyclononane-derived ligands,<sup>12b</sup> has led us to extend this approach to imidazole-based systems. As an initial target, we chose to synthesize  $L_2$ , a dimeric analogue of the recently reported Lippard system,<sup>9</sup>  $L_1$ , which has proved effective in stabilizing both iron(II) and iron(III) dimers.

Ligand  $L_2$  was easily prepared in a two-step, high-yield synthetic sequence. Methylimidazole was deprotonated with butyllithium, and the resulting anion was quenched with 0.5 equiv of benzoyl chloride, giving bis(1-methylimidazol-2-yl)phenylcarbinol (**1**). This carbinol was then treated with sodium hydride in dimethylformamide and reacted with  $\alpha, \alpha'$ -dibromo-*m*-xylene to give the tetraimidazole ligand ( $L_2$ ) in 73% overall yield.

**Metal Complex Formation.** The diiron core was formed by using either of two methods. Stirring a 2:1 mixture of ferrous formate dihydrate and  $L_2$  in methanol under argon gave a clear, colorless solution. After exposure to air, the solvent was removed in vacuo, leaving a green solid. Alternatively, a similar green solid was prepared by the addition of 2 equiv of ferric chloride and excess ammonium formate to a methanol solution of  $L_2$ . The methanol was removed in vacuo, chloroform was added, and the colorless, insoluble salts were filtered off, giving a green solution. Removal of the chloroform in vacuo results in a green solid that was identical in all respects to that formed from ferrous formate. Vapor diffusion of ether into a chloroform/methanol solution of

(13) Rhoda, R. N.; Fraiolo, A. V. *Inorg. Synth.* 1953, 4, 159-160.

(14) Sessler, J. L.; Sibert, J. W.; Hugdahl, J. D.; Lynch, V. *Inorg. Chem.* 1989, 28, 1417-1419.

(15) Lippard, S. J. *Angew. Chem., Int. Ed. Engl.* 1988, 27, 344-361 and references cited therein.

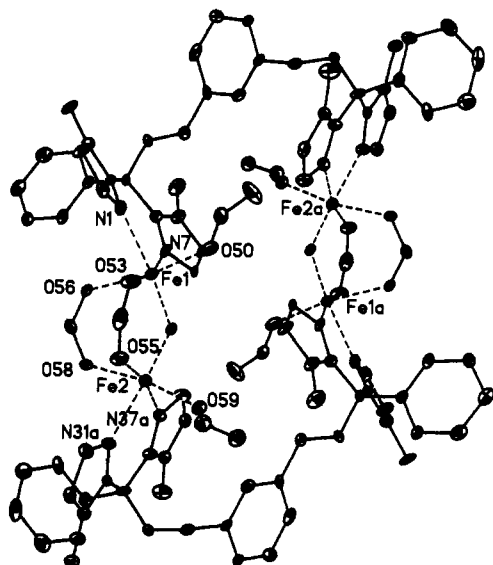


**Figure 1.** View of  $[\text{Fe}_4\text{O}_2(\text{C}_{76}\text{N}_{16}\text{O}_4)(\text{CHO}_2)_8]$ . H atoms are omitted for clarity. Ellipsoids scaled to the 20% probability level. The complex lies around an inversion center located between the Fe dimers. The coordination around each Fe is octahedral and is indicated by the dashed lines. The Fe atoms in the dimer are bridged by two formates and an oxide with an Fe-Fe separation of 3.221 (2) Å. Each Fe is also coordinated by two imidazole nitrogens and a monodentate formate. Relevant Fe bond lengths (Å) are as follows: Fe1-N1, 2.209 (12); Fe1-N7, 2.111 (11); Fe1-O49, 1.807 (8); Fe1-O50, 2.003 (12); Fe1-O53, 2.058 (11); Fe1-O56, 2.142 (9); Fe2-O49, 1.811 (8); Fe2-O55, 2.057 (11); Fe2-O58, 2.088 (9); Fe2-O59, 2.027 (11); Fe2-N31a, 2.206 (11); Fe2-N37a, 2.115 (11). The Fe-Fe distances between the diiron cores are 7.176 (6) (Fe1-Fe2a) and 7.790 (4) Å (Fe1-Fe1a). Relevant bond angles (deg) are as follows: Fe1-O49-Fe2, 125.9 (5); N1-Fe1-O49, 172.2 (4); O56-Fe1-O50, 170.1 (4); O53-Fe1-N7, 165.6 (4); N1-Fe1-O50, 89.9 (4); N1-Fe1-O53, 84.1 (4); N1-Fe1-O56, 80.7 (4); N1-Fe1-N7, 81.5 (4); O49-Fe1-O56, 92.2 (4); O49-Fe1-O53, 98.9 (4); O49-Fe1-O50, 97.3 (4); O49-Fe1-N7, 95.5 (4); N31a-Fe2-O49, 175.4 (4); N37a-Fe2-O55, 165.4 (4); O58-Fe2-O59, 169.7 (4); N31a-Fe2-O55, 84.0 (4); N31a-Fe2-O58, 82.2 (4); N31a-Fe2-O59, 87.6 (4); N31a-Fe2-N37a, 81.5 (4); O49-Fe2-O59, 96.7 (4); O49-Fe2-O58, 93.5 (4); O49-Fe2-O55, 97.2 (4); O49-Fe2-N37a, 97.2 (4). Atoms labeled with an a are related by  $1-x, -y, -z$ .

the iron complex formed using either of the above processes result in the formation of green crystals of **2**.

The single-crystal X-ray analysis of **2** revealed a tetrameric iron complex  $[\text{Fe}_2\text{O}(\text{O}_2\text{CH})_4\text{L}_2]_2 \cdot 4\text{MeOH} \cdot 2\text{CHCl}_3$ , as shown in Figure 1. The complex contains the familiar  $(\mu\text{-oxo})\text{bis}(\mu\text{-carboxylato})\text{diiron(III)}$  core. Each iron is in an approximate octahedral coordination environment with the outer faces of the diiron core capped by the imidazoles and monodentate formates. Interestingly, the rigid xylylene bridge does not link the iron centers by bridging the  $(\mu\text{-oxo})\text{bis}(\mu\text{-formato})\text{diiron(III)}$  core, as one might expect for dimer formation. Instead the two dinuclear cores are linked via the bridge to form a tetranuclear complex with the distances between the cores found to be 7.176 (6) (Fe1-Fe2a) and 7.790 (4) (Fe1-Fe1a) Å.

The similarity between the monomeric and dimeric imidazole-containing ligands,  $\text{L}_1$  and  $\text{L}_2$ , respectively, makes a comparison of the diiron cores of interest. With the obvious exception that  $\text{L}_2$  stabilizes a tetrameric complex and  $\text{L}_1$ , a dimer, the key features of these two ligand-stabilized complexes are remarkably similar. Table III allows for a comparison between complexes **2**, formed from  $\text{L}_2$ , and **3**  $[\text{Fe}_2(\mu\text{-O})(\mu\text{-O}_2\text{CH})_4(\text{L}_1)_2]$ , the diferric complex of  $\text{L}_1$ .<sup>9</sup> The Fe-Fe distance within the core of **2** (3.221 (2) Å) is slightly longer than that of **3** (3.201 (3) Å) and nearly the same as that of azidomethemerythrin (3.23 Å). A similar result is also seen for the Fe-N bond trans to the  $\mu\text{-oxo}$  bridge. The bond is lengthened slightly in **2** (2.209 (12) Å versus 2.16 (1) Å for **3**) but is still shorter than that of the protein (2.24 Å). An interesting difference between **2** and **3**, however, is seen in the positioning of the monodentate formates. The end-on formates in complex

**Table III.** Structural and Spectroscopic Data for **2**, **3**, and Azidomethemerythrin

	<b>2</b>	<b>3</b>	azidomethemerythrin
Fe-O ( $\mu\text{-oxo}$ ) (avg), Å	1.809 (8)	1.79 (1)	1.79
cis-Fe-N (avg), Å	2.113 (11)	2.12 (2)	2.13
Fe-O ( $\mu\text{-formate}$ ) (avg), Å	2.058 (11), <sup>b</sup> 2.115 (9) <sup>c</sup>	2.06 (1), <sup>b</sup> 2.10 (1) <sup>c</sup>	
Fe-O (end-on formate) (avg), Å	2.015 (12)	2.02 (1)	
trans-Fe-N (avg), Å	2.209 (12)	2.16 (1)	2.24
Fe-Fe within core, Å	3.221 (2)	3.201 (3)	3.23
Fe-O-Fe, deg	125.9 (5)	127.0 (6)	130
$\lambda_{\text{max}}$ , nm ( $\epsilon_{\text{M}}/\text{Fe}$ , $\text{cm}^{-1}\text{mol}^{-1}$ ) <sup>a</sup>	662 (8) 518 (sh) 482 (sh, 350) 448 (sh, 370) 356 (sh, 3100) 332 (3350)	662 (70) 520 (sh) 478 (sh) 448 (370) 354 (sh, 2900) 329 (3400)	680 (95)   446 (1850) 380 (sh) 326 (3375)
refs	this work	9	2, 3

<sup>a</sup>Solvent for **2** and **3**, chloroform. <sup>b</sup>Cis to end-on formate. <sup>c</sup>Trans to end-on formate.

**3** are found to lie on opposite sides of a plane drawn through the Fe-O-Fe center, whereas, in **2**, the formates are constrained by the ligand to sit in a cis disposition.

In conclusion, we have synthesized a new ligand capable of binding two metals in a biomimetic environment. The formation of a tetrameric iron(III) complex suggests that dimeric metal complexes are not ensured by the use of rigid linkers. In the present case, it is possible that the 2 H of the xylene bridge is sufficient to inhibit dimer formation and that a directing influence, such as a phenoxide bridge, may be necessary to coerce the irons into forming a dimer.<sup>16</sup> We are presently synthesizing ligands that may allow us to explore such a possibility.

**Acknowledgment.** We are grateful to the National Institutes of Health (Grant No. GM 36348) for financial support of this research.

**Supplementary Material Available:** View of the asymmetric unit, showing the atom labeling scheme, and the unit cell packing diagram (Figures S1 and S2), listings of positional and isotropic thermal parameters for the H atoms (Table S1), anisotropic thermal parameters for the non-hydrogen atoms (Table S2), bond lengths and angles for the non-hydrogen atoms (Tables S3 and S4), and bond lengths and angles for the H atoms (Tables S5 and S6), and an X-ray experimental summary (16 pages); a listing of observed and calculated structure factor amplitudes (Table S7) (24 pages). Ordering information is given on any current masthead page.

(16) Many cases of dimeric metal complexes with bridging phenoxides have been reported. See: Borovik, A. S.; Papaefthymiou, V.; Taylor, L. F.; Anderson, O. P.; Que, L., Jr. *J. Am. Chem. Soc.* **1989**, *111*, 6183-6195 and references cited therein.

Contribution from the Department of Chemistry, University of Houston, Houston, Texas 77204-5641

**Electrochemical, Spectroscopic, and Structural Characterization of  $\text{Rh}_2(\text{dpf})_4$ ,  $\text{Rh}_2(\text{dpf})_4(\text{CH}_3\text{CN})$ , and  $[\text{Rh}_2(\text{dpf})_4(\text{CH}_3\text{CN})]\text{ClO}_4$ , Where  $\text{dpf} = \text{N,N}'\text{-Diphenylformamidinate(1-)}$**

J. L. Bear,\* C.-L. Yao, R. S. Lifsey, J. D. Korp, and K. M. Kadish\*

Received January 30, 1990

Virtually all electron-rich dirhodium(II) tetraamidate or tetraamidate complexes undergo two metal-centered one-electron oxidations.<sup>1-7</sup> Electroreductions of these complexes are generally